Juha-Matti Hirvonen

Spectrally Adjustable Radiance Source

School of Electrical Engineering

Thesis submitted for examination for the degree of Licentiate of Science in Technology.

Espoo, 12.8.2013

Thesis supervisor:

Prof. Erkki Ikonen

Second examiner:

Prof. Liisa Halonen

Thesis advisor:

D.Sc. (Tech.) Petri Kärhä

**Aalto University
School of Electrical
Engineering**

Author: Juha-Matti Hirvonen

Title: Spectrally Adjustable Radiance Source

Date: 12.8.2013   Language: English   Number of pages: 7+33

Department of Signal Processing and Acoustics

Professorship: Measurement Science and Technology   Code: S-108

Supervisor: Prof. Erkki Ikonen

Second examiner: Prof. Liisa Halonen

Advisor: D.Sc. (Tech.) Petri Kärhä

A spectrally adjustable radiance source based on light emitting diodes (LEDs) has been constructed for spectral responsivity measurements of radiance and luminance meters. A 300-mm integrating sphere source with adjustable output port is illuminated using 30 thermally stabilized narrow-band LEDs covering the visible wavelength range of 380–780 nm. The functionality of the measurement setup is demonstrated by measuring the relative spectral responsivities of a luminance meter and a photometer head with cosine-corrected input optics.

Keywords: LED, Radiance source, Spectral responsivity, Photometry

Tekijä: Juha-Matti Hirvonen

Työn nimi: Spektrisesti säädettävä radianssilähde

Päivämäärä: 12.8.2013   Kieli: Englanti   Sivumäärä: 7+33

Valvoja: Prof. Erkki Ikonen

Toinen tarkastaja: Prof. Liisa Halonen

Ohjaaja: TkT Petri Kärhä

Työssä esitellään led-pohjainen spektrisesti säädettävä radianssilähde radianssi- ja luminanssimittareiden spektrisen herkkyyden mittaamiseen. Integroivaa palloa, jonka halkaisija on 300 mm, valaistaan 30 kapeakaistaisella ledillä, joiden aallonpituudet kattavat näkyvän valon aallonpituusalueen 380–780 nm ja joiden lämpötila pidetään vakiona. Mittausasetelman toimivuus esitellään mittaamalla suhteellinen spektrinen herkkyys luminanssimittarille ja fotometrimittapäälle, jossa on kosini-korjattu sisääntulo-optiikka.

Preface

I would like to express my gratitude to (not strictly in order of importance) supervisor professor Erkki Ikonen, second examiner professor Liisa Halonen, advisor Petri Kärhä, colleague Tuomas Poikonen, MRI staff, my wife Anu, my daughter Saara, my mentor Juha and God Almighty.

Otaniemi, 12.8.2013

Juha-Matti Hirvonen

Contents

Symbols and abbreviations

Symbols

$L_{V,M}$ Measured luminance

$L_{V,C}$ Calculated luminance

K_{cd} The conversion coefficient between the watt and the lumen
      ($K_{\mathrm{cd}} = 683 \ \mathrm{lm/W}$)

$L_E(\lambda)$ Spectral radiance

$V(\lambda)$ The efficiency function for photopic vision

$S(\lambda)$ Spectral responsivity

$S_{\mathrm{rel}}(\lambda)$ Relative spectral responsivity

$S_{\mathrm{m}}(\lambda_{\mathrm{eff},i})$ Discrete improved values of $S(\lambda)$

λ_{eff} Effective wavelength

Abbreviations

CIE   International Commission on Illumination

DSR   Differential Spectral Responsivity

DUT   Device Under Test

IR   Infrared

KRISS   Korea Research Intitute of Standards and Science

LED   Light Emitting Diode

NIST   National Institute of Standards and Technology

PMMA   Polymethyl Methacrylate

QTH   Quartz Tungsten Halogen

REF   Reference

UV   Ultraviolet

1   Introduction

Absolute calibrations of colorimeters and luminance meters are usually carried out using a light source with a standardized broadband spectrum, such as the CIE standard illuminant A [1]. These meters are equipped with filters to obtain the spectral responsivity of the standard colorimetric or photometric observer [2, 3]. However, to use the meters reliably for light sources with spectra different from the calibration source, their spectral radiance responsivities have to be known. The responsivities can be measured by using monochromatic or quasi-monochromatic light at different wavelengths. The light source can be based on wideband light such as an incandescent lamp with filters or a monochromator. Alternately, narrow band sources, such as light emitting diodes (LEDs) [4–6] or lasers [7, 8] at different wavelengths can be used.

In order to use the source as a reference in absolute calibrations, the radiant distribution at the output has to be spatially uniform and angularly Lambertian [9]. If the source is used in relative calibrations, then it is enough that the shape of the spectrum remains the same when varying the location and the incidence angle on the radiant surface. The radiant output surface can be reflecting as in integrating spheres [5, 6] or transmitting as with the source pointing on a diffuser plate [4]. With the diffuser plate, masking may be needed to improve the spatial uniformity.

This thesis mainly focuses on a radiance source assembled and reported by Hirvonen *et al* [10]. The source is based on LEDs and an integrating sphere to create a spatially uniform quasi-monochromatic light source. Thirty temperature and current stabilized LED modules are mounted on a carousel that is used for coupling the LEDs one at a time to the input of a 300-mm integrating sphere. The construction of the setup is explained in Section 3. Some earlier work is briefly described in Section 2. Our setup has similarities with the one published by Zaid *et al* [5]. In both sources, the LEDs are mounted on a rotary stage and an integrating sphere is used. However, in our source the LEDs are thermally stabilized and not modulated. The resulting output spectra were measured with a radiance mode spectroradiome-

ter [11], and the stability of the system was determined by measuring the output radiance, block temperature and the forward voltage of the LED over time. The characterization of the radiance source is described in Section 4. It includes measuring the spectrum and the stability of each color channel, and scanning of the spatial uniformity with output apertures of different sizes. The functionality of the source is demonstrated by a spectral responsivity measurement of a luminance meter in Section 5. Methods to analyze the results in order to determine the spectral responsivity of the luminance meter are discussed. The results are analyzed using a method which was presented by Kärhä *et al* [12] for spectral irradiance measurements. Here, we apply it for radiance. Section 5 also covers the uncertainty analysis. The effect of quasimonochromaticy of the LEDs on the measured spectral responsivity is studied by comparison with a monochromator-based reference spectrometer in Section 6.

2 Literature survey

Before making our own radiance source, a literature survey on existing devices was made. The solutions and challenges others have faced with the devices, and the uncertainties expected were of great interest.

The light sources used for deriving the spectral responsivities of imaging meters can be categorized by the way the light is produced (by LEDs, lasers, or incandescent lamps with a monochromator) or by what the radiant output surface is (integrating spheres, or diffusing plates). In this chapter I will briefly go through some published devices and designs.

2.1 Diffuser based calibration light source at Van Swinden Laboratorium

Voigt *et al* [4] have reported a calibration source for photometric devices such as imaging systems or tristimulus sensors built at Van Swinden Laboratorium (VSL) in the Netherlands. The spatial uniformity of the output of the source also enables its usage in measurement of spatial responsivity of an imaging meter. The source is constructed of diffuser plates inside a box and LED modules directed to them. The LED modules consist of separate high power LEDs mounted on black anodized aluminium plates, as seen in Figure 1. The temperatures of the modules are controlled by thermo-electric cooling devices. The modules are attached, one at a time, on an aluminium box, in which the diffuser plates are [Figure 1(b)].

The concept of the box is depicted in Figure 2. The diffuser assembly of the device consists of three diffusers and one masking plate. The first of the diffusers (i.e. the closest to the LEDs) is a single-sided ground glass plate. The third plate, which is in the output, is made of polymethyl methacrylate (PMMA) and it is very diffusive to ensure the Lambertian far field. The second plate between the two is optional. The masking plate between the second and the third diffuser plates is for

flattening the uniformity of the output. The masking is implemented by printing black and white patterns on commercial laser transparencies.

The LEDs in use include Philips Lumileds Luxeon III Lambertian Emitters in colours royal blue (455 nm), green (530 nm) and red (627 nm), and as a second type, Lamina BL3000 Blue Light Engine (470 nm). The achieved luminance level on the output varies between 20.8 cd m^{-2} and 105 cd m^{-2} depending on the source used. The uniformity varies between 96.3 % and 99.1 % depending on the LEDs used. The region of interest in the output is square shaped and the size varies between 16×16 cm^2 and 20×20 cm^2. Voigt *et al* estimate the throughtput of the system to be of the order of 1 %, based on the manufacturer's specifications of the LEDs.
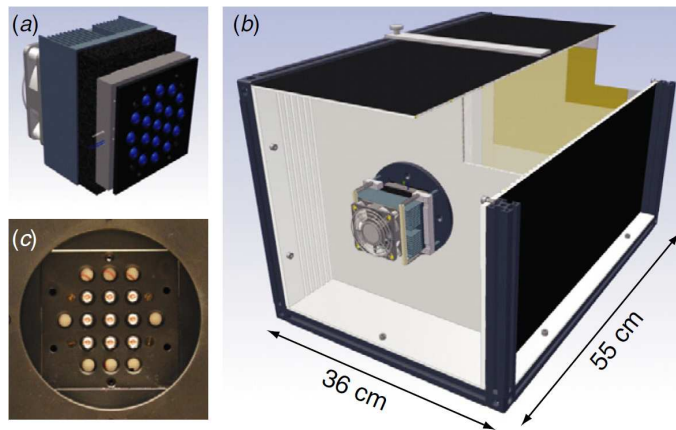

Figure 1: Source design: (a) LED source module, (b) enclosure rear view, (c) high power LED emitter 3×3 square array as configured for experiment [4].
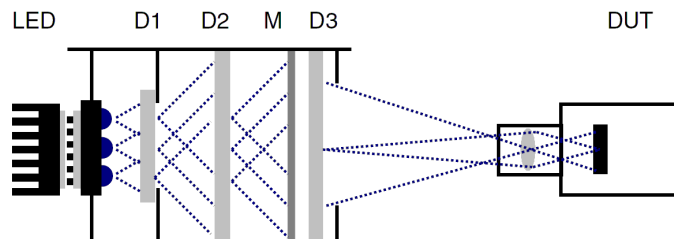

Figure 2: Uniform source concept: stabilized high power LED module (LED), diffusers close to the LEDs (D1) and at the uniform output plane (D3), optional intermediate diffuser (D2), patterned mask (M), device under test (DUT) [4].

2.2 A source based on LEDs and an integrating sphere at Korea Research Institute of Standards and Science

Figure 3 shows schematics of a calibration source developed by the Korea Research Institute of Standards and Science (KRISS) [5]. The device is used for measuring the spectral responsivity of irradiance meters. Due to the bias light of the source, it is possible to measure also the linearity of the meters.
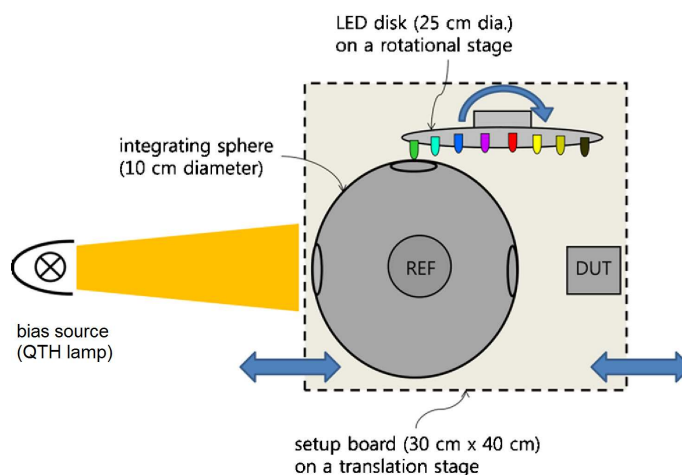

Figure 3: Schematic diagram of the measurement system of spectral responsivity with the tunable LED-based integrating sphere source. Three ports of the sphere are for a quartz tungsten halogen (QTH) incandescent lamp as the bias source, disk of LEDs and the device under test (DUT). The reference detector(REF) is attached in the sphere [5].

The device is based on an integrating sphere and an LED carousel with 35 LEDs. The sphere, as shown in Figure 4, has three ports; one for the bias source, one for the LEDs, and one for the device under test. In the sphere, there is also a photodiode attached as a reference monitor detector. The diameters of the sphere and its output aperture are 100 mm and 40 mm, respectively. The bias source is a quartz tungsten halogen incandescent lamp, and it is used to adjust the irradiance on to a desired level by varying its distance from the sphere. The sphere contains no baffle. The maximum value of the irradiance is 1.5 kW m^{-2}. The minimum level of 300 W m^{-2} is at the distance of 55 cm. The peak wavelengths of the LEDs used in

the setup cover the wavelength range between 280 nm and 1550 nm (Figure 5). The contribution of the LEDs to the spectral irradiance varies between 0.2 mW m^{-2} nm^{-1} and 2 mW m^{-2} nm^{-1}.
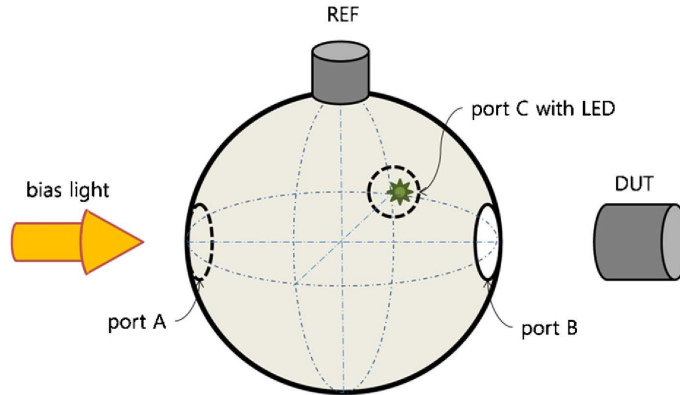

Figure 4: Detailed view of the integrating sphere [5].
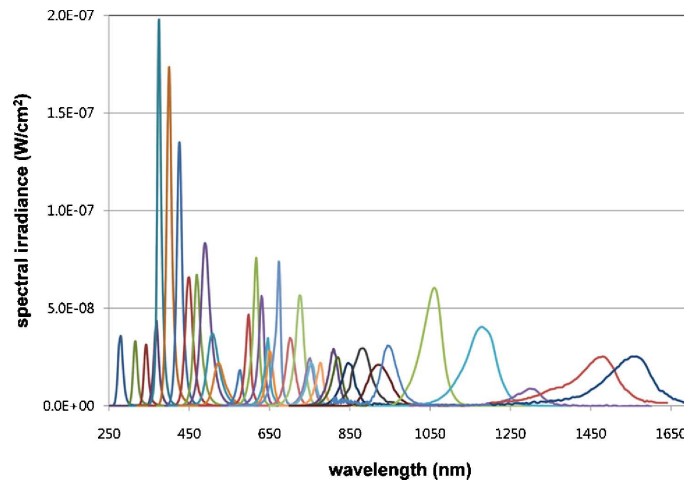
Figure 5: Spectral irradiance of the LED-based integrating sphere source measured at the measurement plane of the DUT with a spectroradiometer. The different colors of the curves correspond to different LEDs, which were selected and lit one by one without modulation [5].

The test detector experiences a radiation field as a superposition of the white component of the bias source and the monochromatic component of the LED. The LEDs are driven with a pulse modulated current, and the component caused by an LED can be derived from the detector signal with a lock-in amplifier. This method

is called the Differential Spectral Responsivity (DSR) method. The modulation frequency can be adjusted between 0.1 Hz and 1 kHz, typically 100 Hz is used. The block diagram of the system is depicted in Figure 6.
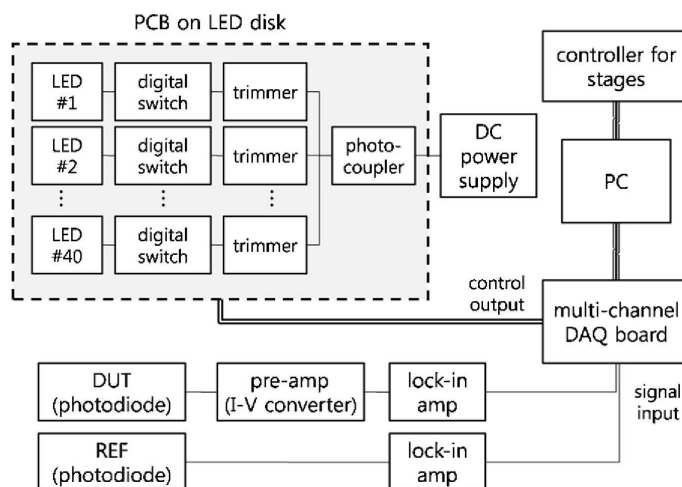

Figure 6: Block diagram of the instrumentation [5].

The main uncertainty components involved in measurement of spectral responsivity of a bare Si detector are repeatability of the reading, reference plane mismatch, calibration of the reference meter and spatial mismatch. The expanded uncertainty ($k = 2$) is 2.2 %.

2.3 Laser based calibration facility at the National Institute of Standards and Technology

The National Institute of Standards and Technology (NIST) has developed a laser-based calibration facility for their facility "Spectral Irradiance and Radiance Calibrations with Uniform Sources" (SIRCUS) [7]. The schematics of the source are shown in Figure 7. The light from a tuneable laser is directed into an integrating sphere through an iris, a vibrating mirror and a lens. The wavelength of the radiation is measured with a wavemeter and the intensity is stabilized with a stabilizer. The vibrating mirror is used to reduce effects caused by the coherence properties of the laser radiation. The purpose of the lens is to improve the spatial uniformity of the

radiance at the exit port of the sphere. The reference detector and the detectors under test are interchanged with a linear translator stage.

There is a variety of integrating spheres ranging in size between 5 cm and 50 cm available. They are also coated with different materials for different applications, such as ultraviolet (UV) and infrared (IR). The lasers used in the setup are Ti-sapphire laser and Nd:YAG laser (neodymium-doped yttrium aluminum garnet). They cover the wavelength range of 200 nm to 1800 nm, details are given in [13]. The standard detector used for wavelengths between 406 nm and 920 nm is a silicon trap detector, which is calibrated against the High Accuracy Cryogenic Radiometer (HACR) [14].

The relative combined standard uncertainties in visible wavelength range are of the order of 10^{-3} in power responsivity measurements and 5×10^{-3} in irradiance responsivity calibrations. Outside the visible region they are between 5×10^{-3} and 10^{-2} in power responsivity, and between 10^{-2} and 2.5×10^{-2} in irradiance responsivity.
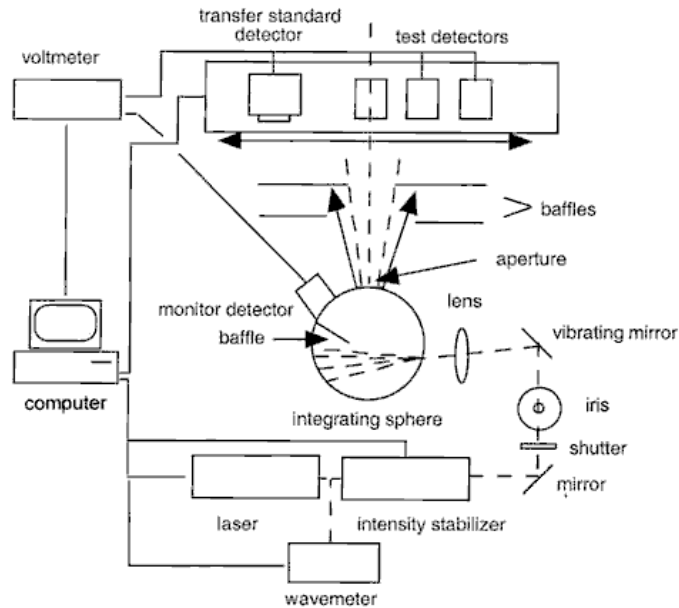

Figure 7: Schematic diagram of the Spectral Irradiance and Radiance Calibration with Uniform Sources (SIRCUS) facility [7].

2.4 Design of an LED-based spectrally tunable source capable of producing any spectral distribution

Fryc *et al* at NIST have designed an LED-based spectrally tunable source [6]. The source produces different kinds of spectra, such as the CIE daylight illuminants, and other common lamp spectral distributions. It also mimicks black body radiator at various temperatures. Thus, it can be used as a standard for spectroradiometric, photometric and colorimetric applications.

Figure 8 shows the structure of the designed source. Number of LEDs, with individual spectral distributions, are mounted on eight to ten LED heads and directed to an integrating sphere. They are driven simultaneously with a 256-channel computer-controlled power supply. The peak wavelengths of the LEDs are between 360 nm and 790 nm (Figure 9). By varying the driving current of each LED, the output spectrum can be adjusted to match the target spectrum using an iterative optimization algorithm. The algorithm is explained in more details in Reference [6].
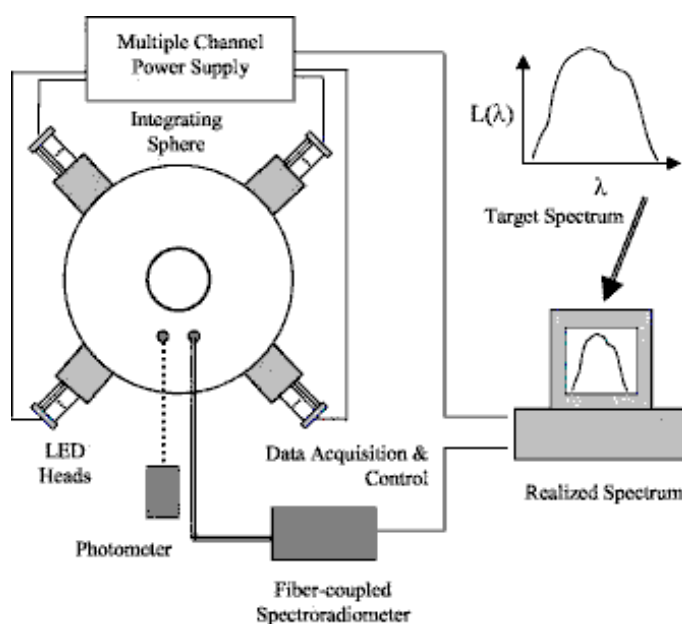
Figure 8: Configuration of the spectrally tunable source designed and being developed at NIST [6].
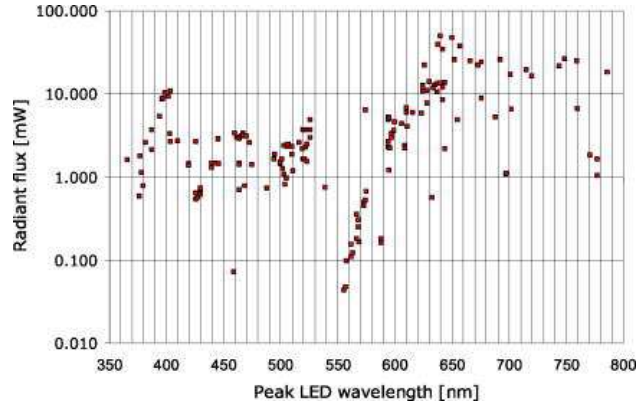
Figure 9: Total radiant flux of the LED samples to be used for the spectrally tunable source, plotted as a function of their peak wavelengths [6].

As an example, Figure 10 shows the target spectra and the expected realizations of (a)illuminant D65 and (b) a white cathode ray tube (CRT) display. Due to the width of the peaks of the LEDs, not all the fine structure of the targeted spectra can be fulfilled. The realization follows the target more precisely, if the structure of the spectrum is smoother.
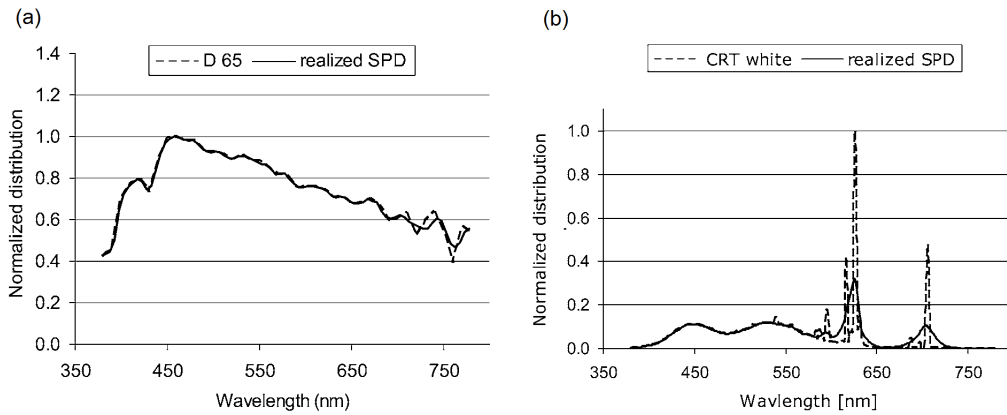
Figure 10: Target spectra (dashed lines) and the expected realizations (solid lines) of (a) illuminant D65 and (b) white cathode ray tube (CRT) display [6].

Fryc *et al* also analyzed measurement accuracies of three different tristimulus colorimeters. According to the results, it seems that by using the tunable source in calibration, the errors in color coordinates x and y values could be an order of magnitude smaller, comparing to calibration with the illuminant A.

3 Measurement setup

3.1 Optical layout

The radiance source constructed in this work is shown in Figure 11. A 300-mm integrating sphere is used with a large area baffle between the input and output ports, as can be seen in the cross-sectional view in Figure 12. A gap of 10 mm between the edge of the baffle and the inner surface of the sphere forms a ring-shaped light source in the output side of the sphere. The input and output ports have diameters of 50 mm and 100 mm, respectively. The diameter of the output port can be reduced down to 16 mm by using apertures of different sizes. In a typical application, a 40-mm aperture is used. Above the output port, there is a cosine-corrected Si-detector for monitoring the stability of the source intensity. The integrating sphere is commercially available from Gigahertz-Optik. The coating material is $BaSO_4$ with surface reflectance of 97 %. The commercial name is (ODP97).

The LED source consists of 30 LED modules and a round aluminium carousel plate mounted on a rotary stage. The diameter of the carousel plate is 460 mm and its mass is around 8.5 kg. The LED modules consist of aluminium blocks and one to four LEDs installed with a mounting plate inside the blocks, as seen in Figure 12. The LED modules are kept at constant temperature with Peltier elements that transfer the heat from the modules to the carousel plate. The rotary stage is used for coupling the LED modules, one at a time, to the input port of the sphere.

The LEDs were chosen so that they have narrow bandwidths and they cover the visible wavelength range of 380 nm – 780 nm. Single color LEDs were preferred when they were reasonably available. The rest of the wavelengths were achieved using white or single color LEDs together with band-pass filters.

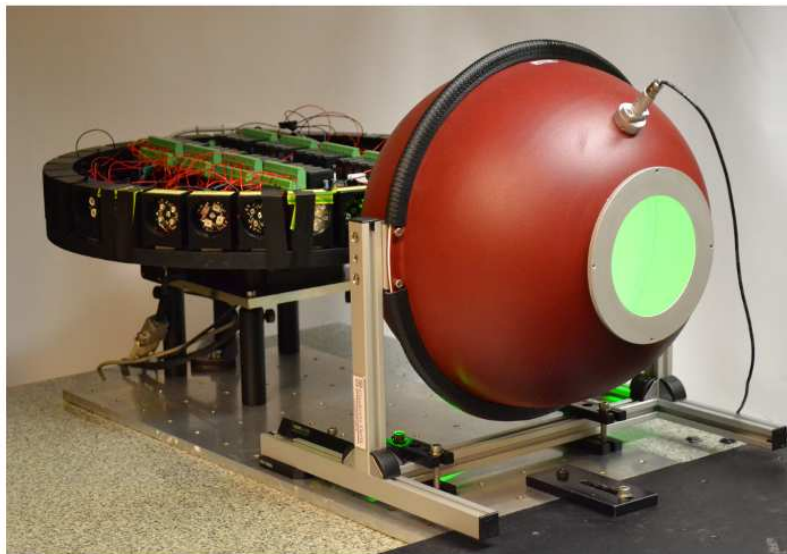Figure 11: Photograph of the spectral radiance source constructed in this work. The carousel containing the individual LED modules is located behind the sphere.
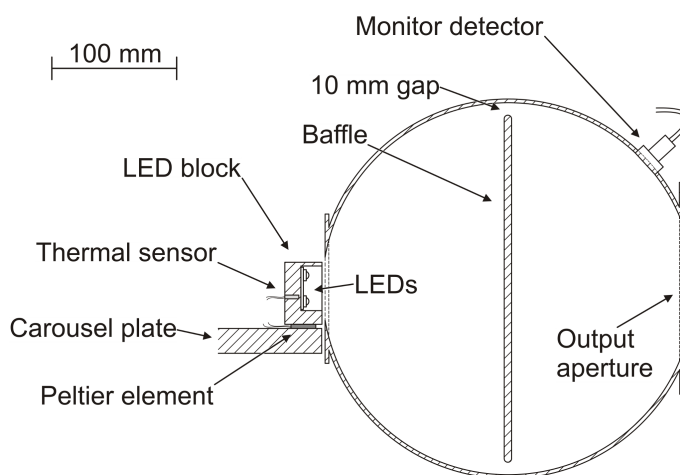

Figure 12: Cross-sectional view of the radiance source. The LED modules are mounted inside aluminium blocks on a round carousel plate, with one module at a time pointing to the sphere. The temperatures of the aluminium blocks are controlled using Peltier elements.

3.2   Temperature control and electronics

Due to the fact that the intensity and the peak wavelength of an LED are sensitive to its junction temperature, the temperatures of the LEDs need to be stabilized [15]. Each LED module has an AD590 -thermal sensor mounted close to the LED inside the aluminium block, and a Peltier element between the module and the plate. The carousel plate works as a heat sink and a thermal capacitor. Only one of the LED modules is used at a time, so the heat capasity of the plate is adequate for the purpose. The blocks are attached to the carousel plate with nylon screws in order to reduce thermal conductance. Every LED block is $30 \times 40 \times 50$ mm^3 in size. With the embedding hole, the mass of each block is about 100 g and the heat capasity is 90 J/K.

To control the LED modules, two 32-channel relay boards, one with single pole relays and the other with double pole relays, are used. The connection diagram is presented in Figure 13. The relay boards are used in parallel, so that each channel connects one LED to a current driver, and both the thermal sensor and the Peltier element to a proportional-integral-derivative (PID) temperature controller. The LEDs are driven with a constant current of 350 mA. Possible voltage peaks are prevented by using bypass-channels with resistive dummy loads for currents when switching between the LED-modules. The rotary stage is a Newmark System model RT5-M17 which is controlled by NSC-1 Series motion controller.

3.3   Software

The device is operated with a computer running LabVIEW$^{\text{TM}}$, and it is fully automated. The relations between the components of the measurement setup can be seen in Figure 14. The procedure of the measurement goes as follows:

1. Rotate the carousel to the desired position

2. Switch on the bypass channel
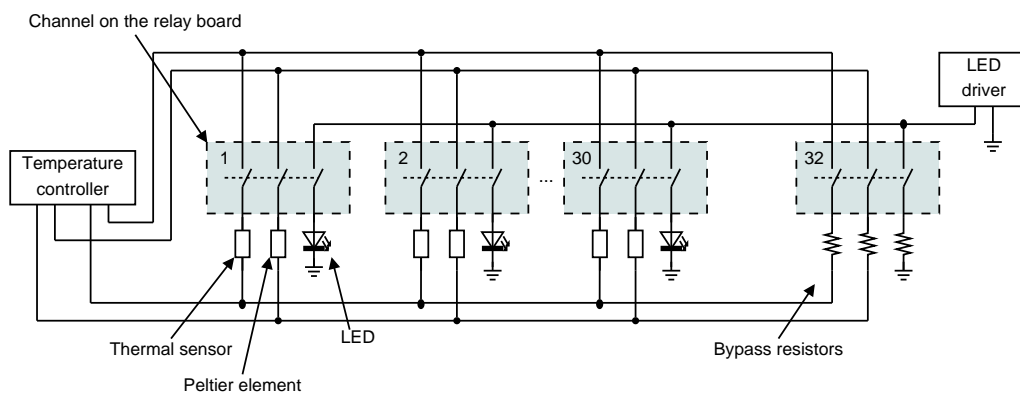
Figure 13: Connection diagram of the LED electronics. Channels 1 to 30 are used for connecting the LEDs to the current driver, and the Peltier elements and the thermal sensors to the temperature controller. Channel 32 is used as a bypass to prevent open loop of the current source and the temperature controller during the change. Channel 31 is not used.
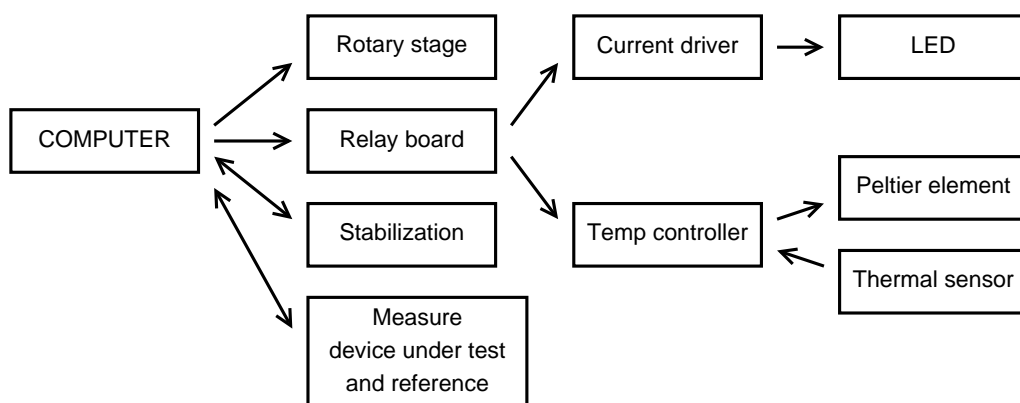
Figure 14: Block diagram of the measurement setup.

3. Switch off the previous channel (if it was on)

4. Switch on the next channel

5. Switch off the bypass channel

6. Measure intensity level with monitor detector

7. Wait until the LED is stabilized

8. Measure with the device under test

9. Measure the spectral radiance with the reference device

10. Repeat from 1. until all LEDs are measured

One sequence takes typically two to five minutes, depending on the LED. Measurement of the luminance and the spectral radiance of each channel takes only a few seconds. The complete measurement round with all channels takes roughly 2.5 hours. The results of the measurements are analyzed with MATLAB.

4 Characterization of the source

4.1 Spectral radiance

The spectral radiance at the output port of the constructed sphere with each LED module was measured using a Konica Minolta CS-2000A spectroradiometer. The results are shown in Figure 15. For clarity, the figure is divided into two subfigures, with the single colour LEDs that have higher intensity in Figure 15 (a), and the filtered white LEDs and lower intensity single color LEDs in Figure 15 (b).

During the measurements, the signal readings of the monitor detector were recorded. The relative spectra of the LEDs do not change between different measurements, if the temperature is the same. Therefore, it is possible to use the monitor detector signal with the measured spectra as a reference in the calibrations.

The array-based spectroradiometer CS-2000A, used in measurements, has a grating to guide the different wavelengths to the ccd-array. Due to the reflections inside the spectroradiometer, there is straylight inside the instrument that can be seen at wavelengths with low signal from the source [16, 17]. The straylight was of the order of 10 nW sr^{-1} m^{-2} nm^{-1} throughout the wavelength range of 380 – 780 nm. The integration time used in the measurements did not affect the straylight level. The effect of straylight has to be corrected from the measurements, because it would distort the calculations with the luminance meter. The errors are largest with UV and IR LEDs, because $V(\lambda)$ emphasizes the values at wavelengths close to its peak at 555 nm.

The distorted parts of the spectra were modelled with exponential functions. Generally the shape of the slope of the LED is considered to be exponential on the blue side and square root on the red side of the peak [18]. However, with our LEDs, the exponential functions fitted best on both slopes, and were therefore used. Figure 16 shows as an example on how the effect of straylight was reduced with a blue LED.
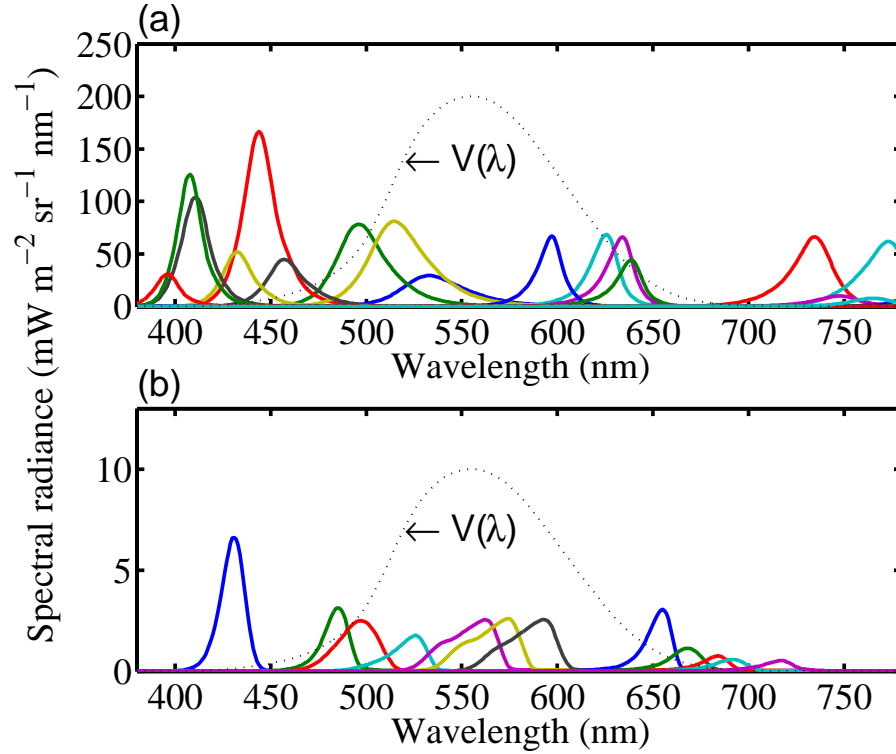
Figure 15: Spectral radiances at the output port produced by modules of higher intensity single color LEDs (a), and modules of filtered white LEDs and lower intensity single color LEDs (b). For comparison, the $V(\lambda)$ curve (in arbitrary units) is also shown.

4.2 Stability of intensity, voltage and temperature

The stabilization of the LED modules was studied by measuring the intensities as well as the junction voltages of the LEDs, and the temperatures of the aluminium LED blocks. The stabilization of temperatures and intensities of two different LED modules is presented in Figure 17. The LED module in Figure 17 (a) has two LEDs with a peak wavelength of 634 nm and a total electrical power consumption of 1.8 W. The LED module in Figure 17 (b) is a white 4-chip LED with a bandpass filter. It has a peak wavelength of 655 nm and an electrical power consumption of 4.2 W.

In the stability measurement, the LED current and the thermal control of the LED block were switched on at the time $t = 0$. The signal of the monitor detector,

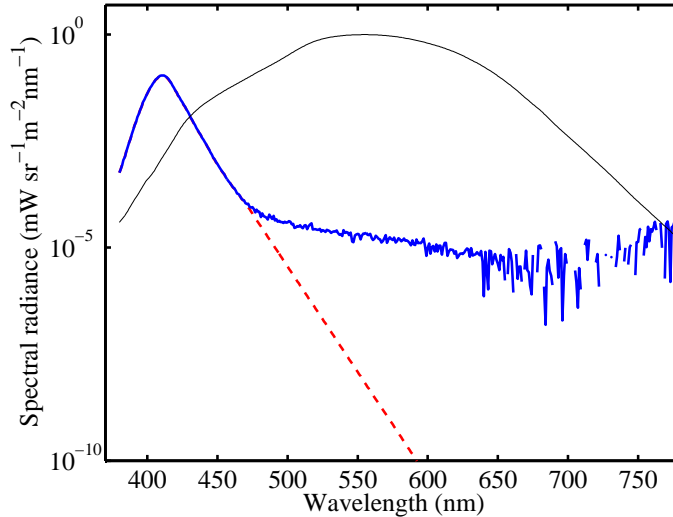Figure 16: Spectrum of a UV-LED with a peak wavelength of 411 nm as measured (solid) and with noise removed mathematically (dashed). The $V(\lambda)$ is depicted as thin line.

the voltage over the LED module and the current through the thermal sensor were recorded. The current through the sensor is proportional to the absolute temperature of the sensor, thus giving the temperature of the LED block.

At constant current, the forward voltage of the LED is shown to be approximately directly proportional to the temperature of the p-n junction of the LED [19]. In our characterization, the temperature behaviour of the LED was derived from its forward voltage as $T_j \sim -V_f$. The junction temperature reaches its thermal equilibrium in 90 seconds, after which it follows the changes of the block temperature.

It was defined that a stable condition of the LED module was achieved, when the relative standard deviation of the monitor signal over 40 seconds was smaller than 0.03 %. According to this definition, the stabilization time of both LED modules (a) and (b) was 3.2 minutes. A typical stabilization time for the LEDs of the source is two to five minutes. The final value, at which the temperatures stabilize, is 26.7 °C, which is the adjusted temperature of 300 K of the temperature controller.
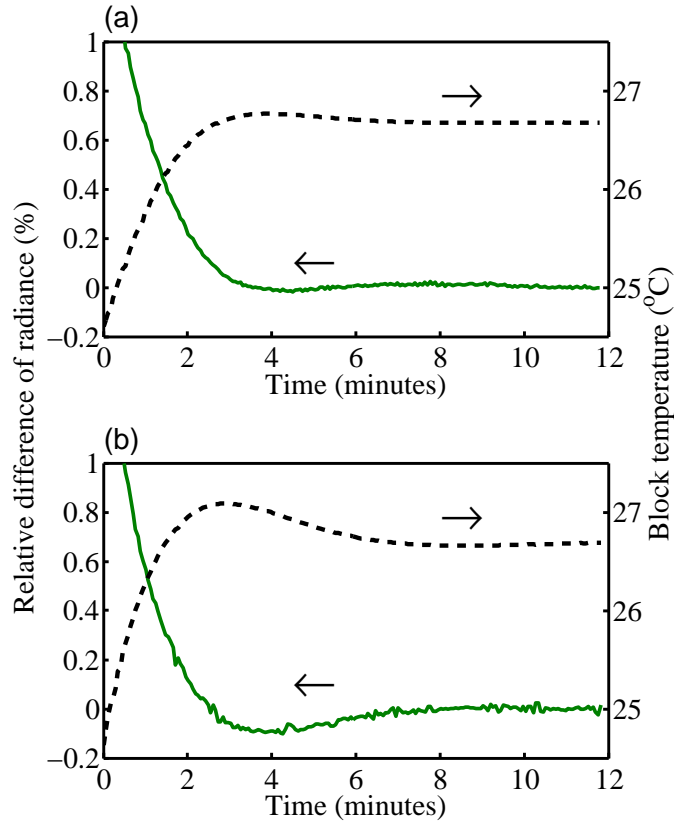
Figure 17: Stabilization of intensity of an LED (solid) and the temperature of the LED block (dashed) after a step change of LED current and turning on the temperature controller. (a) A single color LED and (b) a white LED with a band-pass filter. The intensity of the LED is derived as the signal of the monitor detector and it is shown as percentage deviation from its final value.

4.3   Spatial uniformity

A luminance meter measures average luminance over the area limited by the set solid angle. In absolute calibrations, both the device under calibration and the reference meter should see the same luminance in order to achieve comparable results. However, the meters may have different measuring angles, and the spatial alignment has uncertainty. The spatial uniformity of the sphere output was measured in order to calculate corrections and to estimate uncertainties due to geometrical differences.

The uniformity was scanned with a luminance meter on an xy-translator using

the LED module with a wavelength of 496 nm as the light source. The step size in both horizontal and vertical directions was 5 mm. The measuring cone angle of the luminance meter was 0.33°, and the distance between the meter and the aperture plane of the sphere was 75 cm. Thus, the diameter of the area of the measurement was 4.4 mm. The output was scanned using sphere apertures with diameters of 100 mm, 75 mm and 50 mm.

The results of the uniformity measurements in the horizontal direction can be seen in Figure 18. The data are presented as relative differences from the luminance measured at the center of the aperture. The luminance measured on the port surface is higher close to the edges of the port than at the center. With the 100 mm aperture, the difference between the minimum and the maximum luminances is of the order of 2.5 %, with the 75 mm aperture it is less than 1 %, and with the 50 mm aperture less than 0.5 %. The results in vertical direction are similar.
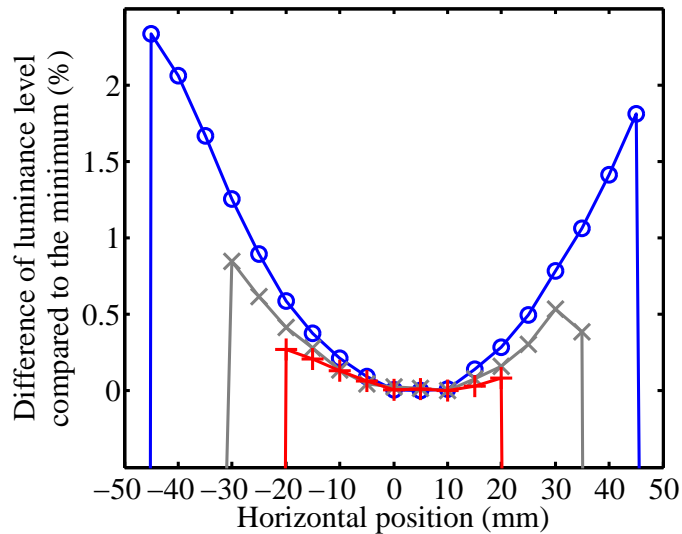
Figure 18: Spatial uniformity of the sphere measured in the horizontal direction at the wavelength of 496 nm with sphere aperture of 100 mm (circles), 75 mm (crosses) and 50 mm (plus signs) normalized to the minimum at the center.

The measurements of the spatial uniformity were repeated with LEDs at the wavelengths of 444, 533, 597 and 639 nm. The measured uniformities differed by less than 0.14 % from the results obtained at the wavelength of 496 nm.

5 Measurement of the relative spectral responsivity of a luminance meter

In order to demonstrate the capabilities of our setup, the relative spectral responsivity of a luminance meter LMT L 1009 was studied. The absolute luminance responsivity of the meter is calibrated against a trap detector with the illuminant A as the spectrum of the light source, using method described by Toivanen *et al* [11].

The luminance $L_{V,i}$ produced by each LED module i was measured with the luminance meter, and the spectral radiance $L_{E,i}(\lambda)$ was measured with a Konica Minolta CS-2000A spectroradiometer used as a reference. The meters were aligned simultaneously on the output of the sphere, close to each other with a viewing angle difference smaller than 10 degrees. Below, it is explained, how the results and their uncertainties were analyzed.

5.1 Analysis of the results

Luminance is defined as [3]

$$L_V = K_{\mathrm{cd}} \int_{\lambda} L_E(\lambda)\, V(\lambda)\, d\lambda, \qquad (1)$$

where $K_{\mathrm{cd}} = 683$ lm/W is the conversion coefficient between the watt and the lumen, $L_E(\lambda)$ is the spectral radiance and $V(\lambda)$ is the efficiency function for photopic vision. In a practical luminance meter, the spectral responsivity $S(\lambda)$ of the meter is matched as closely as possible to $V(\lambda) \cdot K_{\mathrm{cd}}$. Thus the luminance $L_{V,M,i}$ that is measured with the luminance meter, can also be expressed in terms of $L_{E,i}(\lambda)$ as calculated luminance

$$L_{V,C,i} = \int_{\lambda} L_{E,i}(\lambda)\, S(\lambda)\, d\lambda. \qquad (2)$$

The spectral responsivity $S(\lambda)$ is solved recursively starting from suitable initial values, e.g. $V(\lambda) \cdot K_{\mathrm{cd}}$. Luminances $L_{V,C,i}$ are then calculated from the measured spectral radiances $L_{E,i}(\lambda)$ by Equation 2. For each LED measurement we calculate

an effective wavelength $\lambda_{\text{eff},i}$ as

$$\lambda_{\text{eff},i} = \frac{\int_\lambda \lambda\; L_{E,i}(\lambda)\; S(\lambda)\; d\lambda}{\int_\lambda L_{E,i}(\lambda)\; S(\lambda)\; d\lambda}, \tag{3}$$

which is a weighted mean of the wavelength of the spectral radiance, using the spectral responsivity function $S(\lambda)$ as the weighting factor. In the calculation of $\lambda_{\text{eff},i}$ only the shape of the spectrum affects on the effective wavelength.

Improved values for the spectral responsivity at the effective wavelengths $\lambda_{\text{eff},i}$, are obtained by

$$S_{\text{m}}(\lambda_{\text{eff},i}) = \frac{L_{V,i,M}}{L_{V,i,C}} \cdot S(\lambda_{\text{eff},i}). \tag{4}$$

The effective wavelengths are here used as wavelengths at which the discrete values $S_{\text{m}}(\lambda_{\text{eff},i})$ are located. The discrete values are next interpolated to obtain an improved estimate for the continuous function $S(\lambda)$.

The interpolation is done with MATLAB curve fitting toolbox. The tails of the curve are modelled with exponential functions, and the peak with MATLAB smoothing spline function, which minimizes the second derivative of the function and the square sum of distance of the spline curve from the given points. The smoothing parameter used is 0.096. With the obtained $S(\lambda)$ the calculation is repeated from Equation 2. The iteration is repeated until the curve converges to a final solution, for which ten rounds is sufficient. Finally the spectral responsivity $S(\lambda)$ is made relative spectral responsivity $S_{\text{rel}}(\lambda)$ and thus comparable to the $V(\lambda)$ by normalizing it to the value of 1 at the wavelength of 555 nm.

The resulting relative spectral responsivity of the luminance meter is shown in Figure 19. The wavelength range is divided with lines into five regions for uncertainty evaluation, according to the relative deviation Δ of the curve fit. The categories are $\Delta < 0.2$ %, 0.2 % $< \Delta < 2$ % and $\Delta > 2$ %, of which the regions 0.2 % $< \Delta < 2$ % and $\Delta > 2$ % occur on both sides of the peak. Standard deviations are used as the uncertainty components of modeling.

The obtained relative spectral responsivity is compared with ideal $V(\lambda)$ in Figure 20. The quality factor f_1' of the obtained relative spectral responsivity, calculated
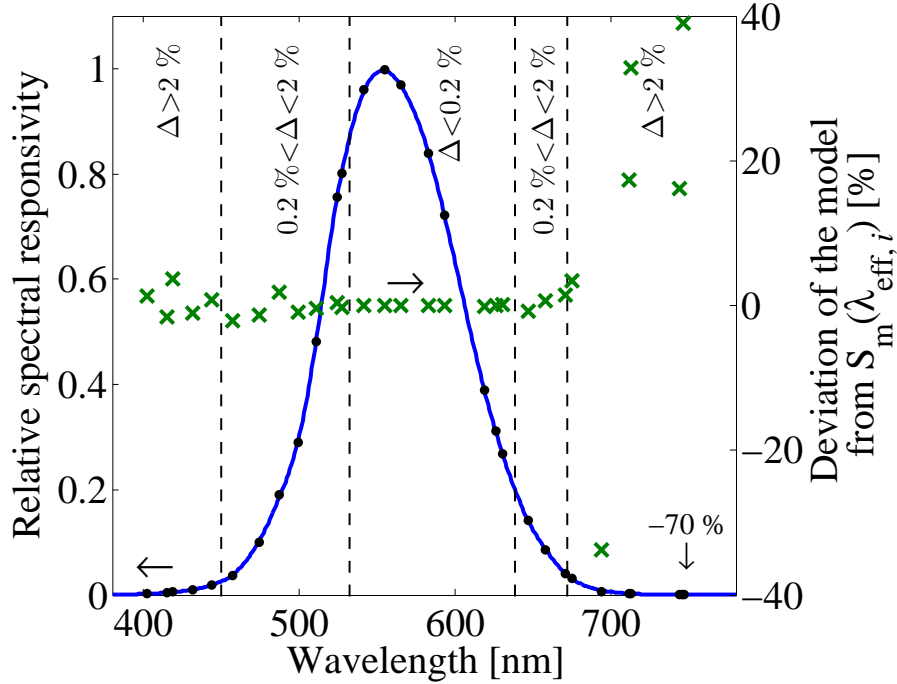
Figure 19: Obtained discrete relative spectral responsivities at effective wavelengths (dots) and the fitted curve (solid line). The crosses indicate their percentage deviation. One point at the wavelength of 748 nm has a value of -70 % and is therefore out of the chart. The wavelength range is divided into five regions according to how much the curve deviates from the points.

according to the CIE 69 [9], is 2.3 %.

The straylight affects the luminance values calculated from the spectral radiances. Luminances $L_{V,C,i}$ in Equation 2 were calculated using the spectral radiances corrected for straylight. The order of magnitude of the straylight correction is less than 0.5 % for wavelengths between 480 nm and 740 nm.

5.2 Uncertainty analysis

The uncertainty budget of the relative spectral responsivity measurement of the luminance meter is presented in Table 1. The uncertainties vary with wavelength. The values shown are examples at the wavelengths of 472 nm, 511 nm, 555 nm, 619 nm
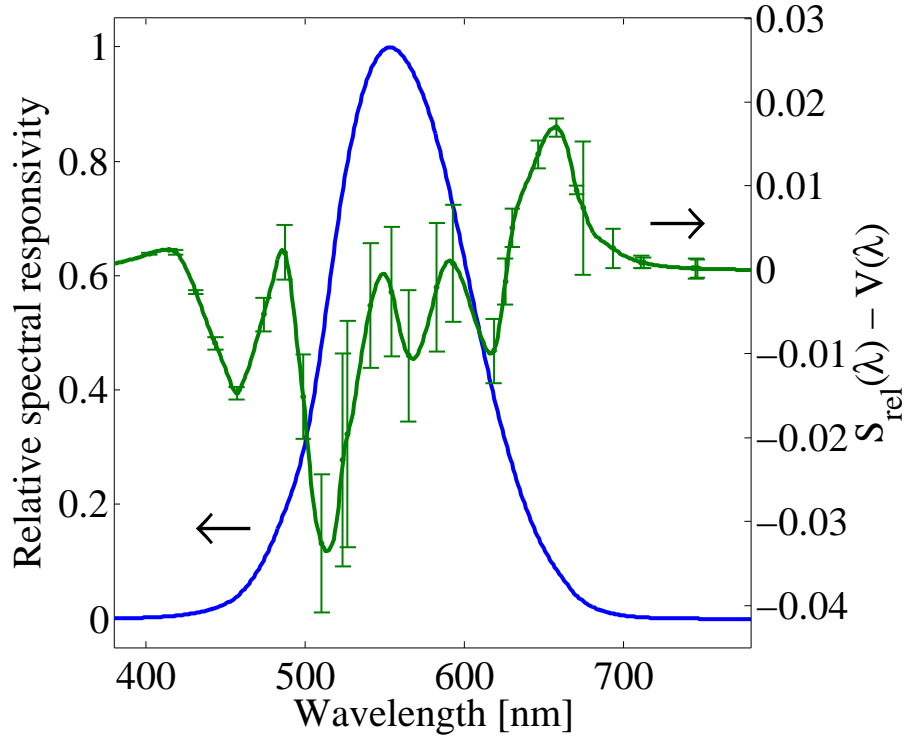
Figure 20: Measured relative spectral responsivity of the LMT L 1009 luminance meter and its deviation from the $V(\lambda)$ curve (right axis). The uncertainties are drawn with a coverage factor $k = 2$.

and 657 nm. The uncertainties in the table are presented in percents as relative uncertainties of the relative spectral responsivity $S_{rel}(\lambda)$, except the values on the last row, which are the expanded absolute uncertainties, i.e. they are multiplied by the value of $S_{rel}(\lambda)$ at each wavelength.

The spectral radiance responsivity of the spectroradiometer, used as the reference, is traceable to the spectral radiance scale of the Metrology Research Institute [11]. The uncertainty of the spectral radiance scale is 0.3 % at 540 nm. Transfer uncertainty due to repeatibility has been included in the values.

The wavelength uncertainty of the reference spectroradiometer is 0.05 nm ($k = 1$). The corresponding standard uncertainty of the relative spectral responsivity was obtained by calculating the change in $S_{rel}(\lambda)$ caused by such a wavelength shift.

Spectral responsivities were analysed using straylight corrected spectral radi-

ances for the LEDs, as explained in Section 4.1. Remaining uncertainties were estimated to be one third of the corrections. Straylight contributes both to the spectral responsivity values and the effective wavelengths as stated. Wavelength uncertainties were converted to uncertainties in responsivity by using the derivative of the spectral responsivity curve.

The resolution of the luminance meter is 1 mcd m^{-2} and its maximum contribution to the uncertainty is 2.6 % at the wavelength of 765 nm. At the wavelengths in Table 1 the uncertainty is <0.01 %, except at the wavelength of 657 nm it is 0.02 %.

In order to derive the effect of the incident angle on the results, the spectral radiance at the center of the aperture was measured in two directions with the difference in incidence angle of 10 degrees. The contribution to the relative responsivity uncertainty is 0.1 %. The uncertainty due to the spatial nonuniformity is less than 0.01 %, since the meters were aligned to the same spot.

Standard deviations of the discrete and interpolated spectral responsivities are used as uncertainties of the measurement and analysis method. The wavelength range was divided into five regions according to the order of magnitude of the deviation as explained with Figure 19.

As expected, the relative uncertainty is bigger at the wavelengths with lower value of the $S_{\mathrm{rel}}(\lambda)$. However, the absolute uncertainty has bigger values close to the peak of the $S_{\mathrm{rel}}(\lambda)$ at the wavelength of 555 nm.

Table 1: Uncertainty budget of the relative responsivity of the luminance meter at five wavelengths. The absolute values on the lowest row have been obtained by multiplying the relative uncertainties by $V(\lambda)$.

Wavelength [nm]	472	511	555	619	657
Value of $V(\lambda)$	0.10	0.52	1.00	0.40	0.07
Source of uncertainty	Relative standard uncertainty [%]				
Spectral radiance responsivity	0.42	0.38	0.37	0.39	0.40
Wavelength scale of the reference meter	0.14	0.10	<0.01	0.09	0.15
Straylight correction, $L_{V,i}$	0.39	0.01	0.02	0.27	0.12
Straylight correction, $\lambda_{\mathrm{eff},i}$	0.06	<0.01	<0.01	0.04	<0.01
Resolution of the DUT	<0.01	<0.01	<0.01	<0.01	0.02
Incident angle	0.10	0.10	0.10	0.10	0.10
Spatial non-uniformity	<0.01	<0.01	<0.01	<0.01	<0.01
Analysis method	0.75	0.75	0.06	0.06	0.40
Combined relative uncertainty	0.96	0.85	0.39	0.49	0.61
Expanded relative uncertainty ($k = 2$)	1.92	1.70	0.77	0.98	1.21
Expanded absolute uncertainty ($k = 2$)	0.0021	0.0088	0.0077	0.0039	0.0008

6 Comparison with a monochromator-based setup

The new radiance source was validated in a comparison with a monochromator-based reference spectrometer [20]. Relative spectral responsivity of an illuminance meter was measured with both devices, and the results were compared.

The reference spectrometer is based on a single monochromator with a bandwidth of 2 nm, and it used a calibrated trap detector as a reference. The photometer was calibrated in under-fill mode for power responsivity. With the radiance source, the photometer head was aligned on the optical axis of the setup at a distance of 50 cm from the output port of the sphere. The quantity measured was thus relative irradiance responsivity in over-fill mode. Both spectral responsivities obtained were normalized to unity at the wavelength of 555 nm to enable comparison.

As seen in Figure 21, the results of the measurements agree within uncertainties. However, due to the bandwidth of the LEDs, some of the fine structure of the spectral responsivity data is averaged. As a result, the f_1' values obtained for the photometer head using the LED source and the monochromator are 1.4 % and 1.9 %, respectively.
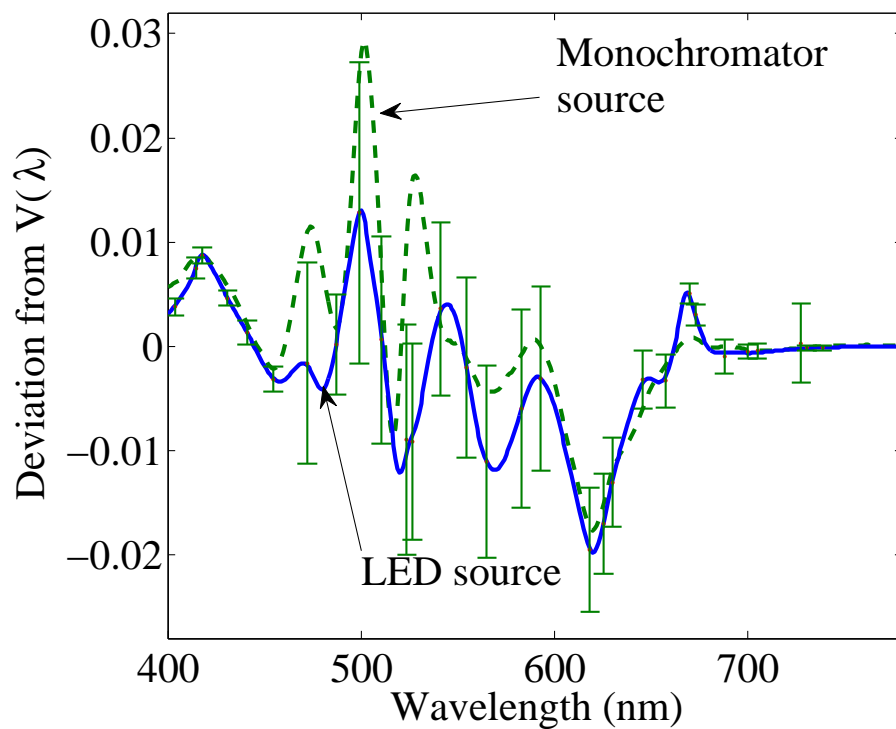
Figure 21: Relative spectral responsivity of a photometer head was measured using the LED-based radiance source (solid line) and a monochromator-based spectrometer setup (dashed line). This figure shows how the responsivities deviate from the $V(\lambda)$ curve. The uncertainties ($k = 2$) include the uncertainties of both methods.

7 Conclusions

A spectrally adjustable radiance source for calibration of radiance meters and luminance meters is presented. The visible wavelength range of $380 - 780$ nm is covered with 30 color channels produced using single-color LEDs and filtered white or single-color LEDs. The temperature of the LED-modules is stabilized using Peltier elements for obtaining stable spectrum and intensity for each color channel. The mechanical structure of the source is modular and the LEDs can be replaced.

The spectra and the stabilization times of the LED modules of the source were thoroughly characterized. The spectral radiances, measured with the spectroradiometer, were distorted by straylight, which was corrected by fitting curves to the distorted parts. Use of a monochromator based spectroradiometer would decrease this effect, but measuring one spectrum would then take up to twenty minutes, compared to the few seconds with the ccd-based spectroradiometer.

The radiance source was tested by measuring the relative spectral responsivity of a luminance meter. The quality factor f_1' obtained for the luminance meter is 2.3 %, and the relative uncertainty of the spectral responsivity at the wavelength of 555 nm is 0.82 % ($k = 2$). Due to the bandwidths of the LEDs, the spectral responsivity is averaged over the spectral bands of the LEDs. The averaging may hide the possible fine structure of the responsivity. A method for analysing the results and the uncertainties of the measurement was presented. The method takes into account the non-monochromaticity of the LEDs.

The effect of the quasi-monochromaticity of the source was tested in a comparison with a monochromator-based setup by measuring the relative spectral responsivity of an illuminance meter. Due to the differences in the bandwidths, the f_1' values obtained using the LED source and the monochromator were 1.4 % and 1.9 %, respectively. Although some of the finest structure of the responsivity is averaged, the number of LEDs of the source is sufficient for characterizing the relative spectral responsivities of luminance meters and illuminance meters within the visible

wavelength range.

The method explained in this thesis also works with other weighting functions, the $V(\lambda)$ function just needs to be replaced with the appropriate function.

References

[1] *CIE standard illuminants for colorimetry.* Number 10526. ISO, Geneva, 1999.

[2] *CIE Colorimetry - Part 1: Standard Colorimetric Observers.* ISO 11664-1:2007(E)/CIE S 014-1/E:2006.

[3] The basis of physical photometry. Technical Report 018.2, International Commission on Illumination, 1983.

[4] D. Voigt, I. A. Hagendoorn, and E. W. M. van der Ham. Compact large-area uniform colour-selectable calibration light source. *Metrologia*, 46(4):S243–S247, 2009.

[5] G. Zaid, S.-N. Park, S. Park, and D.-H. Lee. Differential spectral responsivity measurement of photovoltaic detectors with a light-emitting-diode-based integrating sphere source. *Appl. Opt.*, 49(35):6772–6783, 2010.

[6] I. Fryc, S. W. Brown, G. P. Eppeldauer, and Y. Ohno. Led-based spectrally tunable source for radiometric, photometric, and colorimetric applications. *Optical Engineering*, 44(11):111309, 2005.

[7] S. W. Brown, G. P. Eppeldauer, and K. R. Lykke. Nist facility for spectral irradiance and radiance responsivity calibrations with uniform sources. *Metrologia*, 37(5):579–582, 2000.

[8] M. Noorma, P. Toivanen, F. Manoocheri, and E. Ikonen. Characterization of filter radiometers with a wavelength-tunable laser source. *Metrologia*, 40(1):S220–S223, 2003.

[9] Methods of characterizing illuminance meters and luminance meters: Performance, characteristics and specifications. Technical Report 069, International Commission on Illumination, 1987.

[10] J.-M. Hirvonen, T. Poikonen, A. Vaskuri, P. Kärhä, and E. Ikonen. Spectrally adjustable quasi-monochromatic radiance source based on leds and its applica-

tion for measuring spectral responsivity of a luminance meter. *Measurement Science and Technology*, 2013. Submitted.

[11] P. Toivanen, J. Hovila, P. Kärhä, and E. Ikonen. Realizations of the units of luminance and spectral radiance at the HUT. *Metrologia*, 37(5):527–530, 2000.

[12] P. Kärhä, P. Toivanen, F. Manoochehri, and E. Ikonen. Development of a detector-based absolute spectral irradiance scale in the 380–900-nm spectral range. *Appl. Opt.*, 36(34):8909–8918, 1997.

[13] K. R. Lykke, P.-S. Shaw, L. M. Hanssen, and G. P. Eppeldauer. Development of a monochromatic, uniform source facility for calibration of radiance and irradiance detectors from 0.2 μm to 12 μm. *Metrologia*, 35(4):479–484, 1998.

[14] T. R. Gentile, J. M. Houston, J. E. Hardis, C. L. Cromer, and A. C. Parr. National institute of standards andtechnology high-accuracy cryogenic radiometer. *Appl. Opt.*, 35(7):1056–1068.

[15] S. Chhajed, Y. Xi, Y.-L. Li, Th. Gessmann, and E. F. Schubert. Influence of junction temperature on chromaticity and color-rendering properties of trichromatic white-light sources based on light-emitting diodes. *Journal of Applied Physics*, 97(5):054506, 2005.

[16] S. Nevas, M. Lindemann, A. Sperling, A. Teuber, and R. Maass. Colorimetry of leds with array spectroradiometers. *MAPAN*, 24:153–162, 2009.

[17] S. G. R. Salim, N. P. Fox, E. Theocharous, T. S., and K. T. V. Grattan. Temperature and nonlinearity corrections for a photodiode array spectrometer used in the field. *Appl. Opt.*, 50(6):866–875, 2011.

[18] E. F. Schubert, T. Gessmann, and J. K. Kim. *Light Emitting Diodes*. John Wiley & Sons, Inc., 2000.

[19] Y. Xi and E. F. Schubert. Junction-temperature measurement in GaN ultraviolet light-emitting diodes using diode forward voltage method. *Applied Physics Letters*, 85(13):2163–2165, 2004.

[20] F. Manoochehri, P. Kärhä, L. Palva, P. Toivanen, A. Haapalinna, and E. Ikonen. Characterisation of optical detectors using high-accuracy instruments. *Analytica Chimica Acta*, 380(2–3):327–337, 1999.